Characterization of an eag-like potassium channel in human neuroblastoma cells

Roman Meyer and Stefan H. Heinemann

Max Planck Society, Research Unit Molecular and Cellular Biophysics, Drackendorfer Strasse 1, D-07747 Jena, Germany

(Received 19 August 1997; accepted after revision 3 December 1997)

1. SH-SY5Y human neuroblastoma cells were investigated with whole-cell and perforated patch recording methods.

2. Besides a quickly activating delayed rectifier channel and a HERG-like channel, a slowly activating potassium channel with biophysical properties identical to those of rat eag (r-eag) channels was detected, here referred to as h-eag.

3. h-eag shows a marked Cole–Moore shift, i.e. the activation kinetics become very slow when the depolarization starts from a very negative holding potential. In addition, extracellular Mg^{2+} and Ni^{2+} strongly slow down activation.

4. Application of acetylcholine induces a fast block of the current when recorded in the perforated patch mode. This block is presumably mediated by Ca^{2+}, as about 1 μM intracellular Ca^{2+} completely abolished h-eag outward current.

5. When cells were grown in the presence of 10 μM retinoic acid in order to synchronize the cell line in the G1 phase of the cell cycle, h-eag current was reduced to less than 5% of the control value, while the delayed rectifier channel was expressed more abundantly. Down-regulation of h-eag by long-term exposure to retinoic acid was paralleled by a right shift in the activation potential of HERG-like channels.

6. Acute application of 10 μM retinoic acid blocked the delayed rectifier channel but enhanced the h-eag current.

7. Thus, our results show that human neuroblastoma cells express in a cell cycle-dependent manner an $[Mg^{2+}]_o$-dependent potassium channel (h-eag) which is blocked by submicromolar concentrations of intracellular Ca^{2+}.

Potassium channels (K^+ channels) play a major role in the electrical signalling of excitable cells and they also appear to be involved in the process of cell proliferation (e.g. Dubois & Rozaire-Dubois, 1993; Wonderlin & Strobl, 1996). The advent of molecular cloning techniques has revealed a wide variety of K^+ channel proteins which show diverse functional properties, albeit having quite homologous primary structures. Owing to the progress of molecular biology, K^+ channels have been isolated and characterized in heterologous expression systems prior to their identification in native tissues. One of these examples is r-eag (Ludwig *et al.* 1994), the rat homologue of the ether-à-go-go K^+ channel. This channel, when expressed in *Xenopus* oocytes or mammalian cell lines, shows remarkable functional properties. The activation kinetics upon depolarizing voltage steps slow down considerably when the holding potential is very negative; in addition, activation slows down further in the presence of extracellular Mg^{2+} in the millimolar range (Terlau, Ludwig, Steffan, Pongs, Stühmer & Heinemann, 1996). Moreover, r-eag channels are potently inhibited by intracellular Ca^{2+}, which makes them sensitive towards muscarinic stimulation which triggers the release of Ca^{2+} from intracellular stores (Stansfeld *et al.* 1996). In addition, the channel may play a potential role in cell proliferation, as r-eag channel currents are absent in cells previously incubated with mitosis-promoting factors (Brüggemann, Stühmer & Pardo, 1997).

In this study, we investigated the electrophysiological properties of SH-SY5Y human neuroblastoma cells. For these cells it was reported that the expression of the human *eag*-related gene channel (HERG) undergoes variations in the voltage threshold for activation during the cell cycle, being potentially responsible for the observed changes in the cell resting potential (Arcangeli *et al.* 1995). Besides HERG, we identified in these cells a K^+ current component which shares properties of currents mediated by heterologously expressed r-eag channels, including voltage-dependent activation kinetics, sensitivity towards extracellular Mg^{2+} and intracellular Ca^{2+}, as well as cell cycle-dependent regulation.

METHODS

Cell culture

Human neuroblastoma cells (SH-SY5Y, German Collection of Microorganisms and Cell Cultures, Department of Human and Animal Cell Cultures, Braunschweig, Germany) were routinely cultured in Dulbecco's modified Eagle's medium–F12 medium (DMEM–F12; 1 : 1) containing 15% fetal calf serum, and incubated at 37 °C in a humidified atmosphere with 7·5% CO_2. Cells were used 1–8 days after seeding. Retinoic acid (RA) was used for cell synchronization in the G1 phase (Thiele, Reynolds & Israeal, 1985; Arcangeli *et al.* 1995). Cells were cultured in the presence of 10 μM RA for 2 or 3 days before electrophysiological experiments were performed.

Patch-clamp recordings

Currents were measured at room temperature (20–24 °C) with an EPC9 (HEKA Elektronik, Lambrecht, Germany) patch-clamp amplifier. Data acquisition and stimulation were controlled with the program Pulse (HEKA Elektronik). Data were corrected routinely for leak currents and capacitive transients using a P/n method, and series resistance errors were compensated in the range of 50–85%. Most experiments were performed in the whole-cell patch-clamp configuration (Hamill, Marty, Neher, Sakmann & Sigworth, 1981). Patch pipettes were fabricated from Kimax-51 glass (Kimble Glass Inc., Vineland, NJ, USA) with resistance values in the range of 2–7 MΩ. Perforated patch recordings were obtained by the method described by Rae, Cooper, Gates & Watsky (1991). The tip of the pipette was dipped into standard internal solution and the pipette was backfilled with standard internal solution containing, in addition, 0·24 mg ml^{-1} amphotericin B. The series resistance decreased in 5–15 min to values below 50 MΩ.

The programs PulseFit (HEKA Elektronik) and Igor-Pro (WaveMetrics Inc., Lake Oswego, OR, USA) were used for data analysis. The rise time needed to reach 80% of maximal current from the baseline was determined after traces were either low-pass filtered at 100 Hz or idealized with double-exponential fits. Data are given as means ± S.E.M. (n = number of independent experiments), unless stated otherwise.

The rise time of h-eag channel activation (τ_r) as a function of the prepulse voltage (V) (see Fig. 2B) was described by a first-order Boltzmann function:

$$\tau_r(V) = \tau_r(-\infty) - (\tau_r(-\infty) - \tau_r(+\infty))/(1 + \exp(-(V - V_{½})/k)), \quad (1)$$

where $V_{½}$ denotes the mid-point of this distribution and k is a measure for the steepness.

Solutions

The external solution was changed either by total exchange of the bath solution or with an application pipette which was placed directly above the cell. The standard extracellular 40 mM K^+ solution was (mM): 96 NaCl, 40 KCl, 2 $CaCl_2$, 2 $MgCl_2$ and 10 Hepes (pH 7·4). Alternatively, a solution with only 5 mM K^+ was used (mM): 135 NaCl, 5 KCl, 2 $CaCl_2$, 2 $MgCl_2$ and 10 Hepes (pH 7·4). In some cases, extracellular solutions were supplemented with 5 mM glucose and/or 500 nM tetrodotoxin. Solutions with various Mg^{2+} concentrations were mixed from extracellular solutions containing 0 or 10 mM $MgCl_2$. The influence of Ni^{2+} was tested with solutions containing $NiCl_2$ instead of $MgCl_2$. The standard pipette solution was (mM): 130 KCl, 10 NaCl, 2 $MgCl_2$, 10 EGTA and 10 Hepes (pH 7·4). For a few experiments, 2 mM reduced glutathione (GSH) was added to the internal solution, as it reduced the degree of current run-down. An internal solution with 0·83 μM free Ca^{2+} was obtained by addition of 9·3 mM $CaCl_2$ to the standard internal solution. The free Ca^{2+} concentration was calculated based on an algorithm by Harrison & Bers (1987), and stability constants from Martell & Smith (1974). Chemicals were obtained from Sigma, except for amphotericin B and tetrodotoxin (ICN Biochemicals, Aurora, OH, USA).

RESULTS

Whole-cell patch clamp recording revealed a heterogeneous distribution of voltage-gated K^+ currents in SH-SY5Y cells. Besides a previously described channel with characteristics of the human *eag*-related gene channel (HERG) (Arcangeli *et al.* 1995; see also Figs 4 and 6), we found a rapidly activating delayed rectifier channel and another outwardly rectifying channel which activated much more slowly. The current components sometimes occurred simultaneously, but there were many cells which had only one or other component. Such cells were used for a more detailed characterization. As shown in Fig. 1, these two current components can be distinguished quite easily according to their activation kinetics. Although the voltage threshold for activation of both types was around −20 mV, the delayed rectifier channel showed a much more rapid activation than the slow channel. In Fig. 1C the rise time to 80% of the steady-state value is compared for both types, showing that delayed rectifier currents activate more than an order of magnitude faster than the slow channels. Long depolarizations of 2 s duration reveal that the slow channels do not undergo inactivation, while delayed rectifier channels show some degree of slow inactivation (Fig. 1B).

The activation kinetics of the delayed rectifier channel do not depend very strongly on the holding potentials (not shown), while the slow channel exhibits a very pronounced Cole–Moore shift. This is a property which is characteristic of the recently cloned gene encoding the r-eag K^+ channel (Ludwig *et al.* 1994; Terlau *et al.* 1996). Therefore, we are going to refer to the slow current as h-eag current indicating the origin in a *human* cell line. For r-eag channels, it was shown that the slow activation and the Cole–Moore effect are strongly regulated by extracellular Mg^{2+}. Therefore, we measured the activation kinetics of the h-eag channels in various extracellular Mg^{2+} concentrations ($[Mg^{2+}]_o$) using various holding potentials, keeping the concentration of extracellular Ca^{2+} constant at 2 mM. Such data are shown in Fig. 2, indicating that the activation kinetics are slowed down as $[Mg^{2+}]_o$ increases. To quantify this phenomenon, we determined the time required to reach the 80% current level as a function of both $[Mg^{2+}]_o$ and the holding potential (Fig. 2B). The rise time as a function of the holding potential clearly undergoes a transition which was characterized here by a first-order Boltzmann function (eqn (1)). The resulting mid-potentials ($V_{½}$) are plotted in Fig. 2C as a function of $[Mg^{2+}]_o$, showing the summarized Mg^{2+} dependence of the activation kinetics. The transition voltage between fast and slow activation becomes less negative with increasing $[Mg^{2+}]_o$. Similar experiments were performed in the absence of extracellular Mg^{2+}, but with various concentrations of

extracellular Ni^{2+}. An example is shown in the bottom panel of Fig. 2*A*, indicating that 50 μM extracellular Ni^{2+} is even more effective in slowing down the activation of h-eag than 10 mM Mg^{2+} – a similar phenomenon was found for the r-eag channel, expressed in *Xenopus* oocytes (Terlau *et al.* 1996).

The pharmacological profile of the h-eag currents in SH-SY5Y cells was investigated by applying fixed concentrations of quinidine, TEA, or 4-aminopyridine (4-AP) to the bath medium and measuring the steady-state outward currents of both h-eag and the delayed rectifier at +50 mV in standard external solution (see Methods). TEA (10 mM) blocked h-eag by 55·3 ± 1·6% ($n = 6$) and the delayed rectifier by 81·8 ± 2·0% ($n = 6$); 5 mM 4-AP blocked h-eag by 65·1 ± 2·7% ($n = 6$) and the delayed rectifier by 83·5 ± 2·5% ($n = 4$); 5 μM quinidine blocked h-eag by 47·5 ± 3·2% ($n = 4$) and the delayed rectifier by 27·6 ± 3·2% ($n = 4$). As none of these blockers clearly discriminates between h-eag channels and delayed rectifiers, detailed analysis of h-eag currents was performed in those cells which predominantly expressed h-eag channels.

r-eag channels are blocked by intracellular Ca^{2+} at low concentrations (65 nM) and, therefore, they are sensitive to muscarinic stimulation, which results in a rapid release of Ca^{2+} from intracellular stores (Stansfeld *et al.* 1996). Owing to these properties, r-eag channels were speculated to form the molecular basis for M-currents (Stansfeld, Ludwig, Roeper, Weseloh, Brown & Pongs, 1997). As h-eag currents in SH-SY5Y cells showed almost identical biophysical properties to r-eag channels expressed in *Xenopus* oocytes or mammalian cell lines, we performed whole-cell current recordings in the perforated patch mode to monitor the current under voltage-clamp control without strongly affecting the composition of the cytosol. In Fig. 3*A* current recordings of h-eag channels are shown before and shortly after application of 10 μM acetylcholine (ACh) to the bath solution. ACh induces a rapid block of h-eag currents which is readily reversible (Fig. 3*A* and *B*). This effect could, in principle, be mediated by several different pathways such as direct G-protein coupling. We, therefore, performed experiments in which we started a whole-cell recording with a pipette tip filled with solution buffered to a $[Ca^{2+}]_i$ of 0·83 μM; the rest of the pipette was filled with EGTA-

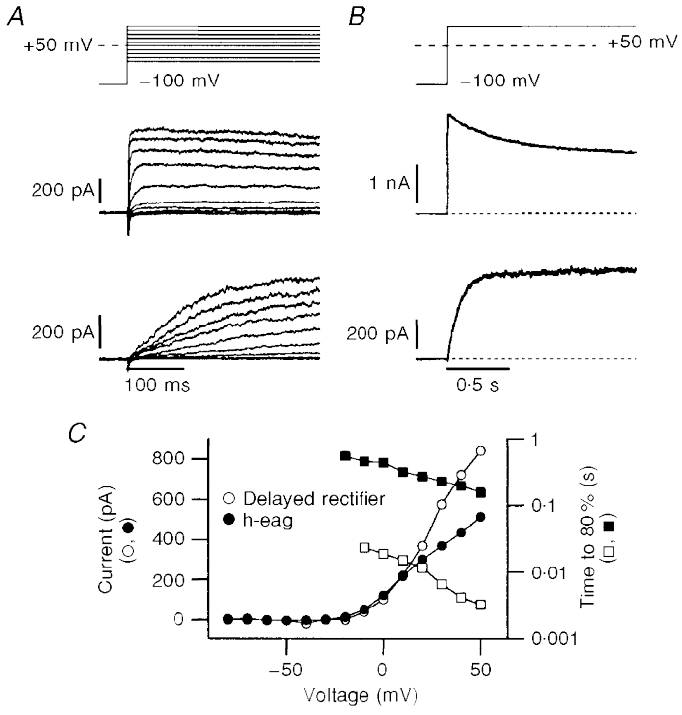

Figure 1. Voltage dependence of h-eag and delayed rectifier currents

A and *B*, examples of whole-cell currents from two different SH-SY5Y cells, elicited with the indicated pulse protocols, showing currents with delayed rectifying characteristics (top) and h-eag currents (bottom). The bath solution contained 2 mM Mg^{2+} and 40 mM K^+ in addition to the standard components (see Methods); the patch pipette was filled with the standard internal Ca^{2+}-free solution. h-eag currents can be distinguished from delayed rectifier currents by the slower time course of activation (*A*) and the lack of inactivation during long depolarizations (*B*). *C*, currents measured at the end of the depolarization phase of the data shown in *A* are plotted as a function of the test potential (○, ●), indicating a similar threshold of activation for delayed rectifier and h-eag channels. In addition, the time to reach 80% of the maximal current after depolarization is plotted on a log scale, indicating the difference in the speed of activation between delayed rectifier (□) and h-eag channels (■). The data points are connected by straight lines.

buffered Ca^{2+}-free saline. After establishing a whole-cell configuration, the solution in the pipette tip quickly equilibrates with the cytosol, effectively suppressing h-eag currents (Fig. 3*C*, pulse 2). Then, a slow equilibration between the solutions in the tip and the rest of the patch pipette takes place, leading to a continuous decrease of $[Ca^{2+}]_i$ to 0 and, hence, an increase in h-eag currents (Fig. 3*C* and *D*). Similar experiments were done in the reverse order (pipette tip filled with Ca^{2+}-free solution, backfilled with solution buffered to a $[Ca^{2+}]_i$ of 0·83 μM), showing converse results, i.e. a decrease in current with time (data not shown). Thus, these experiments show that h-eag channels are effectively blocked by intracellular Ca^{2+} at a concentration significantly lower than 1 μM.

The next question we addressed regards the possible involvement of h-eag in the cell cycle. These experiments were motivated by a report that heterologously expressed r-eag channels can be down-regulated by a mitosis-promoting factor (Brüggemann *et al.* 1997). In addition, studies by Arcangeli *et al.* (1995) have revealed that the HERG-like current observed in SH-SY5Y cells undergoes cell cycle-dependent changes in voltage-dependent activation properties, leading to a stabilization of the resting potential in the G0/1 phase. We, therefore, estimated the quantitative distribution of delayed rectifier channels and h-eag channels by recording whole-cell current with 2 mM Mg^{2+} in the bath, and applied two depolarizations to +50 mV from holding potentials of −60 and −130 mV. Both the time course of activation and the pronounced Cole–Moore shift clearly identify the fraction of h-eag currents in the cells (Fig. 4*A*). HERG-mediated currents were measured at −120 mV after the depolarizing step in the presence of 40 mM extracellular K^+. While both the delayed rectifier channels and h-eag give rise to fast tail currents, the deactivation time course of HERG currents is very slow (see Fig. 4*A*). Therefore, taking the peak of the slowly deactivating tail currents as a measure for HERG expression only yields very little contamination by delayed rectifier and h-eag channels. In a first set of experiments with 5 mM K^+ in the extracellular solution, we found in nineteen control cells that the expression level of h-eag current was similar to that of the delayed rectifier (Fig. 4*B*, Experiment 1). In order to synchronize the cells in the G0/1 phase of the cell cycle, we incubated them for 2–3 days in 10 μM retinoic acid. After this procedure we

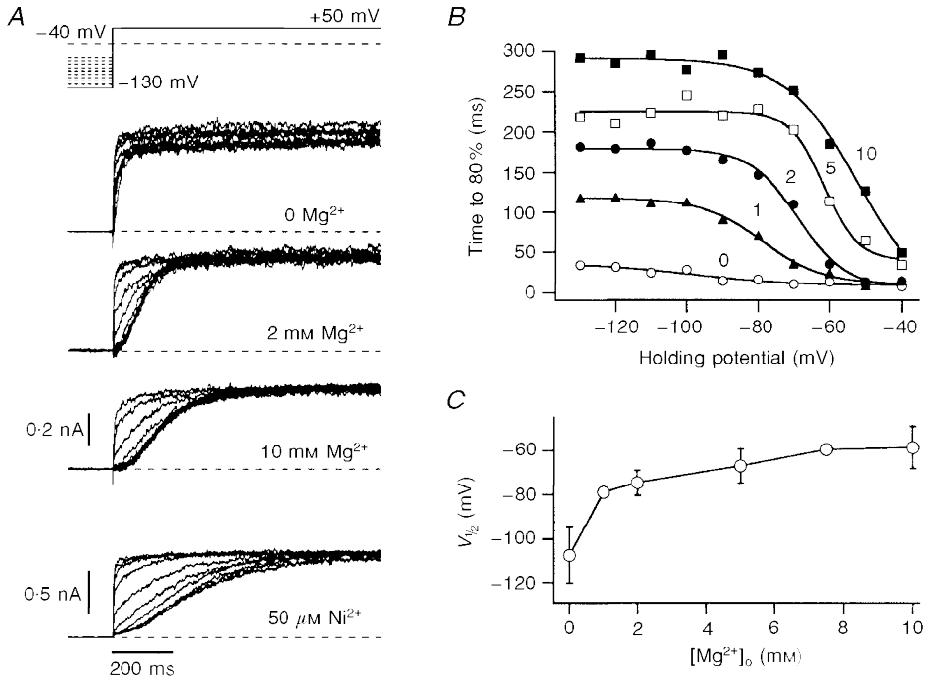

Figure 2. Mg^{2+} and Ni^{2+} dependence of h-eag channel activation

A, the activation kinetics of h-eag channels depend upon the holding potential. Current traces are shown for depolarizations to +50 mV from holding potentials ranging from −130 to −40 mV in steps of 10 mV. While in the first trace the external solution contained only 2 mM Ca^{2+} as divalent cations in the 5 mM K^+ solution, data in the next traces were recorded in external solutions with additional 2 and 10 mM Mg^{2+} and 50 μM Ni^{2+}. The data for Ni^{2+} were obtained from a different cell. *B*, the rise time to 80% of the maximal current was determined from idealized traces (see Methods) and is plotted here *versus* the holding potential for the indicated Mg^{2+} concentrations (mM). The continuous curves are fits according to a first-order Boltzmann equation (eqn (1)), yielding an apparent voltage where the transition between slow and fast activation phases occurs, $V_{½}$. *C*, $V_{½}$ values determined from experiments described in *B* are plotted as a function of the Mg^{2+} concentration. The error bars indicate S.D. values; the data points are connected by straight lines.

recorded twenty-one cells in retinoic acid-free solution and found h-eag currents in only two cells. Simultaneously, the yield of delayed rectifier currents was greater than in the control cells. In order to also assess the expression of HERG currents (at −120 mV), we performed similar experiments with eleven and twenty-five control cells in 40 mM extracellular K^+ (Fig. 4*B*, Experiments 2 and 3). After differentiation of the cells by incubation in retinoic acid, expression of h-eag decreased to negligible values (□), while the expression of delayed rectifier channels increased (■). HERG-mediated current, however, did not markedly change (▨).

As the lack of h-eag currents in retinoic acid-treated cells could possibly be due to a direct effect of residual retinoic acid on the channel rather than a consequence of the selection of cells in the G0/1 phase, we recorded both delayed rectifier currents and h-eag currents, and applied 10 μM retinoic acid to the bath solutions. The result is illustrated in Fig. 5, showing that the delayed rectifier channels (Fig. 5*A*) were blocked (−12·3 ± 2·2%, $n = 6$) while, in contrast, current through h-eag channels (Fig. 5*B*) was increased (+37·2 ± 6·0%, $n = 5$) by retinoic acid. This indicates that the lack of h-eag channels in G0/1 phase cells is unlikely to be caused by a direct effect of retinoic acid on the channels.

As illustrated in Fig. 4, retinoic acid-induced differentiation of SH-SY5Y cells results in a marked down-regulation of h-eag channels, while the expression of delayed rectifier channels is increased. At the same time, K^+ inward currents through HERG channels are not significantly affected. This finding may seem to contrast with the findings of Arcangeli *et al.* (1995) who reported a shift in the activation potential of HERG channels by cell differentiation. However, data shown in Fig. 4 were obtained after depolarizations to +50 mV for 1 s, i.e. under conditions in which the activation of HERG is saturated. Therefore, in addition we determined for the cells of Experiment 3 (see Fig. 4*B*) the voltage dependence of HERG activation by measuring K^+ inward currents at −120 mV after 10 s prepulses to various voltages. This protocol is illustrated in Fig. 6*A*; outward and inward currents of two different cells are shown. Both cells express HERG, but the outward currents are only carried by either h-eag (bottom) or delayed rectifier channels (top). The peak inward current at − 120 mV was plotted as a

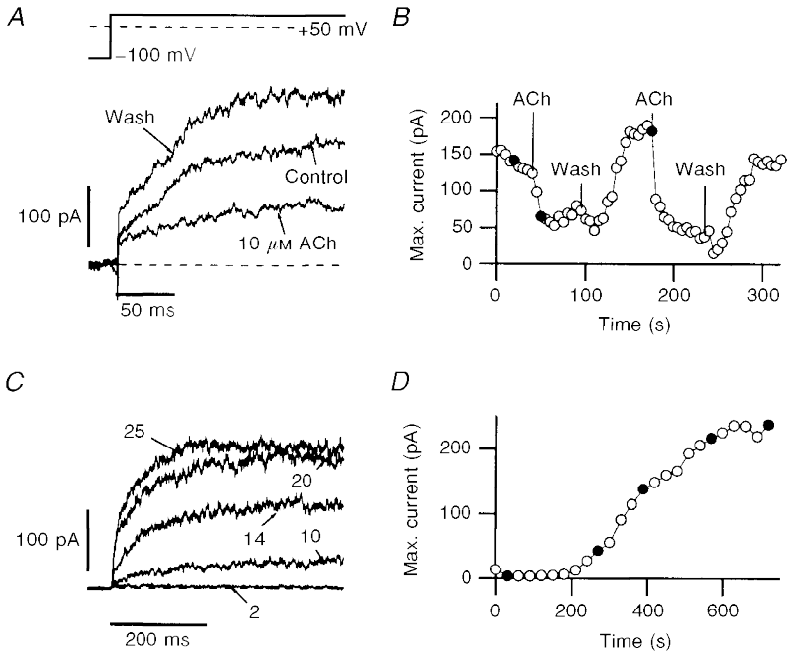

Figure 3. Block of h-eag channels by muscarinic stimulation and intracellular Ca^{2+}

A, current traces recorded with the perforated patch-clamp method. The channels were activated every 5 s by depolarizing steps from −100 to +50 mV. Addition of 10 μM ACh resulted in current decrease in a reversible manner. *B*, the amplitude of the slowly activating current component is plotted as a function of time. The application and removal of 10 μM ACh is indicated. *C*, the influence of internal Ca^{2+} was investigated with the whole-cell patch-clamp method. The tip of the pipette was filled with a solution containing 0·83 μM free Ca^{2+} and the pipette was backfilled with the standard internal EGTA-buffered, Ca^{2+}-free solution. After obtaining a whole-cell configuration, the internal Ca^{2+} concentration rose quickly to about 0·83 μM, leading to a complete channel block, which was assayed by depolarizations to +50 mV, repeated every 20 s. The backfilled Ca^{2+}-free solution then slowly removed the Ca^{2+} from the cell, resulting in full channel activation. *D*, the mean current determined from the plateau phase of the current traces is shown as a function of time. The filled circles in *B* and *D* indicate the data obtained from the traces shown in *A* and *C*, respectively.

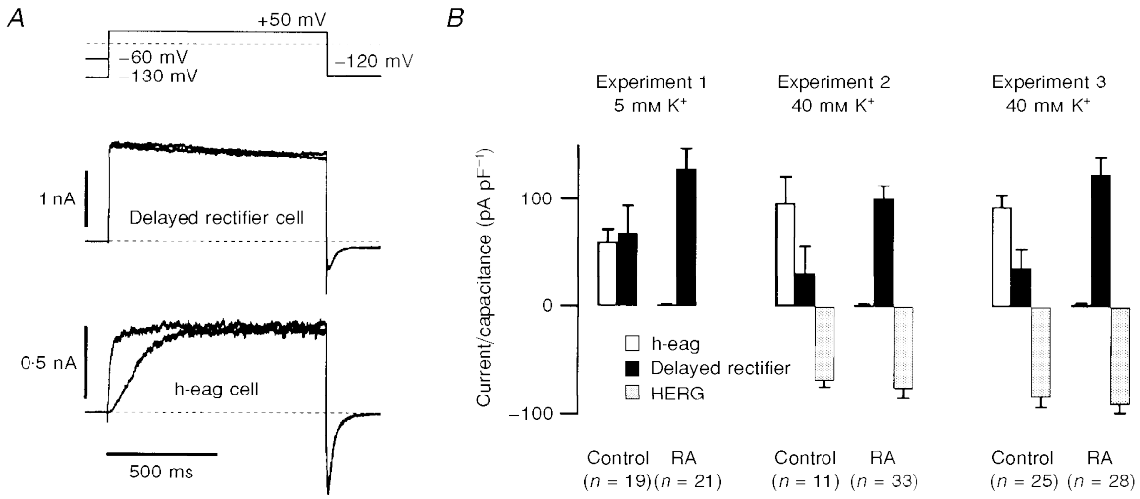

Figure 4. Effects of long-term exposure to retinoic acid

SH-SY5Y cells were cultured under control conditions and in the presence of 10 μM retinoic aicd (RA). *A*, the expression of delayed rectifier or h-eag channels was tested with two pulses to +50 mV from holding potentials of −130 mV and −60 mV. This protocol reveals a clear Cole–Moore shift for h-eag channels (bottom traces) and no change of activation for delayed rectifier channels (top traces). Traces are from different cells. In cells where both channel types were present, h-eag and delayed rectifier components could easily be distinguished due to the different activation kinetics when depolarized from a holding potential of −130 mV. HERG channel expression was assessed by measuring the peak of the slowly deactivating inward K^+ current after the depolarization at −120 mV. A clear discrimination with respect to the other components is possible because HERG channels do not conduct appreciable outward currents owing to a very fast C-type inactivation, and they deactivate much more slowly than other delayed rectifier channels or h-eag (Schönherr & Heinemann, 1996; Smith, Baukrowitz & Yellen, 1996). *B*, h-eag (□), delayed rectifier (■), and HERG currents (▨) normalized to the cell capacitance determined for three sets of experiments without (Control) and after culturing the cells in presence of 10 μM RA for 2 or 3 days (RA). Experiment 1 was performed in 5 mM K^+ extracellular solution; Experiments 2 and 3 were performed in 40 mM K^+ extracellular solution. HERG expression was only assessed in 40 mM K^+ solution.

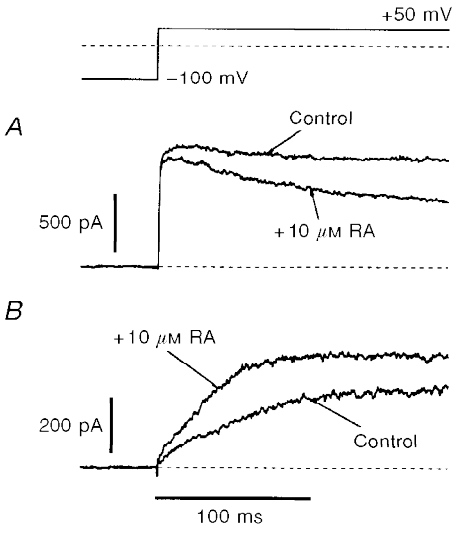

Figure 5. Acute exposure to retinoic acid

The direct effect of RA on h-eag and delayed rectifier channels was investigated in the whole-cell patch-clamp configuration. *A*, delayed rectifier current was blocked after exposure of the cell to 10 μM RA. *B*, in contrast, for h-eag channels a current increase was observed under identical conditions. *A* and *B* show current traces from different cells.

function of the prepulse potential (Fig. 6*B*). A description by a first-order Boltzmann law was used in order to estimate the voltage for half-maximal activation, $V_{½}$. In Fig. 6*C* the cells were distributed into two groups: one group contained cells which only expressed h-eag outward currents (left), and the other group contained those cells which mostly expressed delayed rectifier currents (right). Four cells in which both channel types were present were discarded. Due to the distribution shown in Fig. 4*B* it is obvious that the first group mostly contained cells measured without differentiation by retinoic acid. For the two groups, histograms for the half-maximal activation voltage for HERG were compiled and are shown in Fig. 6*C*. The histograms indicate that expression of h-eag correlates with the activation threshold of HERG, which is more negative in undifferentiated cells.

DISCUSSION

SH-SY5Y human neuroblastoma cells express a variety of K^+ channels. In this report we characterized a current component which shows striking similarities to the currents mediated by cloned r-eag K^+ channels (Ludwig *et al.* 1994) in many biophysical respects. Owing to its origin in a human cell line, we refer to this channel as h-eag. We have shown that the voltage-dependent activation of h-eag strongly depends on the holding potential (Cole–Moore shift) and on the extracellular concentration of Mg^{2+}. Both properties are virtually identical to those reported for r-eag expressed in *Xenopus* oocytes (Terlau *et al.* 1996). Thus, human neuronal cells also possess a K^+ channel which is strongly regulated by extracellular Mg^{2+}, which could provide an alternative way of modulating cell excitability. The strong sensitivity of the channel for divalent cations

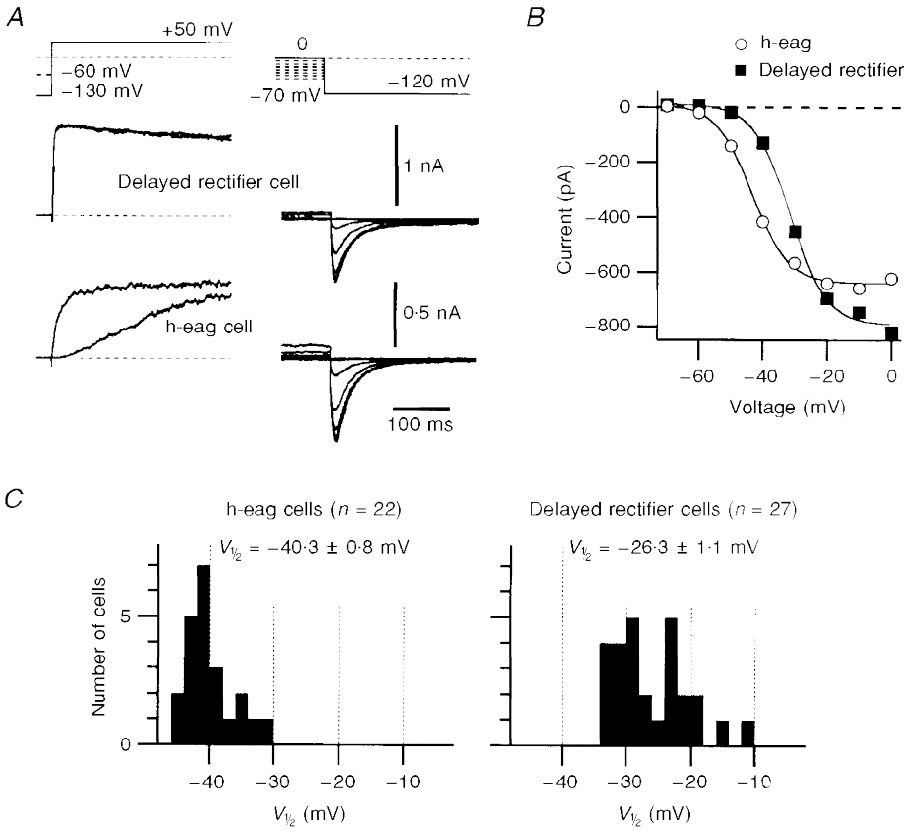

Figure 6. Expression of h-eag correlates with the activation threshold of HERG

A, the expression of h-eag and delayed rectifier currents was assessed by double-pulse protocols to +50 mV from −60 and −130 mV (see also Fig. 4). In the same cells, bathed in 40 mM K^+ solution, activation of HERG channels was determined by depolarizing the cells for 10 s to the indicated voltages and by measuring the resulting tail currents at −120 mV. HERG-mediated currents (right traces) and the corresponding outward currents (left traces) originate from identical cells. *B*, K^+ inward current through HERG channels (see *A*) is plotted as a function of the prepulse potential. ○, currents from the cell which expressed h-eag. ■, currents from the cell which expressed delayed rectifier channels. The continuous curves are first-order Boltzmann fits to the data. *C*, the distribution of half-maximal activation voltages, $V_{½}$, determined from plots as shown in *B* are presented as histograms. For this purpose, cells were divided into two groups: one which expressed h-eag only (left) and one in which only delayed rectifiers contributed to the outward currents (right). The mean values of the $V_{½}$ distributions are indicated.

such as Ni^{2+} may indicate a molecular site responsible for the toxicity of these ions.

Like r-eag channels (Stansfeld *et al.* 1996), h-eag in SH-SY5Y cells is efficiently blocked by intracellular Ca^{2+}. The channel is thereby subject to strong regulation by Ca^{2+}, since the half-maximal blocking concentration is near the basal cytosolic Ca^{2+} concentration. This high Ca^{2+} sensitivity makes the channel sensitive to cell stimulations which liberate Ca^{2+} from internal stores. We tested, as one of many possible pathways, cell stimulation by acetylcholine and found a rapid and reversible reduction of the h-eag current amplitude. Similar experiments performed in the whole-cell configuration with Ca^{2+}-free pipette solution did not result in current reductions (data not shown), indicating that there is no direct effect of ACh or the activated muscarinic receptors on h-eag channels. At present, it cannot be excluded that there may be additional effects of activated muscarinic receptors on h-eag channels to those mediated by Ca^{2+} (e.g. involving diffusible G-protein subunits).

K^+ channels in SH-SY5Y cells are subject to extensive cell cycle-dependent regulations. As reported by Arcangeli *et al.* (1995), an inwardly rectifying channel which shares similarities with the human *eag*-related gene channel (HERG) undergoes variations in voltage-dependent activation during various cell cycles. The authors of this study suggest that the scatter of half-maximal voltage of HERG channel activation is strongly reduced in the G0/1 phase, leading to a stabilization of the resting potential. Here, we show that h-eag channels in SH-SY5Y cells are efficiently suppressed in the G0/1 phase of the cell cycle. Interestingly, a delayed rectifier channel appears to be regulated in the opposite way to the h-eag channel, as it is strongly expressed in G0/1 cells. In cells without treatment with retinoic acid, expression of h-eag channels is more frequent than expression of the delayed rectifier channels. Thus, like HERG channels, h-eag channels may play a role in proliferation of neuronal cells. Interestingly, cloned r-eag channels were reported to be inhibited by mitosis-promoting factors (Brüggemann *et al.* 1997), indicating that r-eag and h-eag show a similar cell cycle regulation.

Arcangeli, A., Bianchi, L., Becchetti, A., Faravelli, L., Coronnello, M., Mini, E., Olivetto, M. & Wanke, E. (1995). A novel inward-rectifying K^+ current with a cell-cycle dependence governs the resting potential of mammalian neuroblastoma cells. *Journal of Physiology* **489**, 455–471.

Brüggemann, A., Stühmer, W. & Pardo, L. A. (1997). Mitosis-promoting factor-mediated suppression of a cloned delayed rectifier potassium channel expressed in *Xenopus* oocytes. *Proceedings of the National Academy of Sciences of the USA* **94**, 537–542.

Dubois, J.-M. & Rouzaire-Dubois, B. (1993). Role of potassium channels in mitogenesis. *Progress in Biophysics and Biology* **49**, 1–21.

Hamill, O. P., Marty, A., Neher, E., Sakmann, B. & Sigworth, F. J. (1981). Improved patch-clamp techniques for high-resolution current recording from cells and cell-free patches. *Pflügers Archiv* **391**, 85–100.

Harrison, S. M. & Bers, D. M. (1987). The effect of temperature and ionic strength on the apparent Ca-affinity of EGTA and the analogous Ca-chelators BAPTA and dibromo-BAPTA. *Biochimica et Biophysica Acta* **925**, 133–143.

Ludwig, J., Terlau, H., Wunder, F., Brüggemann, A., Pardo, L. A., Marquardt, A., Stühmer, W. & Pongs, O. (1994). Functional expression of a rat homologue of the voltage gated ether-à-go-go potassium channel reveals differences in selectivity and activation kinetics between the *Drosophila* channel and its mammalian counterpart. *EMBO Journal* **13**, 4451–4458.

Martell, A. E. & Smith, R. M. (1974). *Critical Stability Constants.* Plenum Press, New York and London.

Rae, J., Cooper, K., Gates, P. & Watsky, M. (1991). Low access resistance perforated patch recordings using amphotericin B. *Journal of Neuroscience Methods* **37**, 15–26.

Schönherr, R. & Heinemann, S. H. (1996). Molecular determinants for activation and inactivation of HERG, a human inward rectifier potassium channel. *Journal of Physiology* **493**, 635–642.

Smith, P. L., Baukrowitz, T. & Yellen, G. (1996). The inward rectification mechanism of HERG cardiac potassium channel. *Nature* **397**, 833–836.

Stansfeld, C. E., Ludwig, J., Roeper, J., Weseloh, R., Brown, D. & Pongs, O. (1997). A physiological role for ether-à-go-go K^+ channels? *Trends in Neurosciences* **20**, 13–14.

Stansfeld, C. E., Röper, J., Ludwig, J., Weseloh, R. M., Marsh, S. J., Brown, D. A. & Pongs, O. (1996). Elevation of intracellular calcium by muscarinic receptor activation induces a block of voltage-activated rat ether-à-go-go channels in a stably transfected cell line. *Proceedings of the National Academy of Sciences of the USA* **93**, 9910–9914.

Terlau, H., Ludwig, J., Steffan, R., Pongs, O., Stühmer, W. & Heinemann, S. H. (1996). Extracellular Mg^{2+} regulates activation of rat eag potassium channel. *Pflügers Archiv* **432**, 301–312.

Thiele, C. J., Reynolds, C. P. & Israeal, M. A. (1985). Decreased expression of N-*myc* precedes retinoic acid-induced morphological differentiation of human neuroblastoma. *Nature* **313**, 404–406.

Wonderlin, W. F. & Strobl, J. S. (1996). Potassium channels, proliferation and G1 progression. *Journal of Membrane Biology* **154**, 91–107.

Acknowledgements

We would like to thank A. Rossner for technical assistance and R. Schönherr for helpful discussions. This work was supported by the Deutsche Forschungsgemeinschaft 'SFB 197, Biological and Model Membranes'.

Corresponding author

S. H. Heinemann: Max Planck Society, Research Unit Molecular and Cellular Biophysics, Drackendorfer Strasse 1, D-07747 Jena, Germany.

Email: ite@rz.uni-jena.de